OPTIMIZATION OF ELECTROLYTIC CELLS

Richard Alkire, See-Aun Soon, and Mark Stadtherr

Department of Chemical Engineering
University of Illinois
Urbana, Illinois 61801

ABSTRACT

A methodology was developed for optimizing electrolytic cells described by a potential field distribution along with material, voltage, and economic balance equations. In the present study, the cell consisted of two flow-through porous electrodes separated by a membrane. The model consisted of two nonlinear differential equations, 19 variables, 8 equality constraints, and 5 inequality constraints. The optimum solutions were obtained for simple economic objectives with use of a successive quadratic programming method. The sensitivity of the optimum to operating variables and design constraints was found with use of Lagrange multipliers. The method may be applied to any electrolytic cell which can be modeled by a combination of differential, algebraic and polynomial (curve-fit) equations.

The modeling of electrochemical systems based on fundamental principles has advanced to a high degree of sophistication in recent years. Such models pave the way for the use of improved techniques for optimizing electrochemical processes. In the present study, a flexible and robust method is used to optimize an electrolytic cell modeled by a set of differential and nonlinear algebraic equations.

The literature on electrochemical optimizaton studies has recently been reviewed [1]. Published works on optimization have generally used an analytical technique in which a cost equation is differentiated with respect to the variable of interest, the derivative set to zero and the equation solved to obtain the optimum value. Another commonly reported approach is use of a graphical technique where the tradeoff curves were plotted and the optimum determined by inspection.

With the advent of the digital computer, the field of optimization has been completely revolutionized. Within the past two decades, there has been a rapid growth in the literature on optimization. There are available several reviews of nonlinear optimization methods [2], applications [3,4], as well as algorithms and software [5,6]. Lasdon [5] has identified the four most promising nonlinear optimization algorithms as the Augmented Lagrangian (AL),

Successive Linear Programming (SLP), Generalized Reduced Gradient (GRG), and Successive Quadratic Programming (SQP). Recent comparative studies have found that GRG and SQP seemed to be the most promising of the four methods.

Modern techniques of optimization are beginning to appear in the electrochemical literature. Alkire, Cera, and Stadtherr [7] implemented a state-of-the-art algorithm for the optimization of an electrolytic cell. They used the GRG method of Lasdon [8] to optimize profit for a chlor-alkali cell based on a model of a diaphragm cell by MacMullin [9]. Current and potential distribution phenomena in the cell, however, were not taken into account because the optimization method used in that study did not lend itself efficiently to applications which involve differential equations. This limitation is removed in the present study.

Models of current and potential distribution within cells have increasingly served as guides in the design, scale-up, and optimization of electrochemical cells. Models of electrolytic cells generally include both nonlinear algebraic and differential equations. In the present work, a general methodology was developed that incorporates state-of-the-art optimization techniques with a model of the current and potential distribution within an electrolytic cell [10]. The goal was to optimize efficiently all cell parameters simultaneously. In this study, a divided cell containing two flow-through porous electrodes was chosen for investigation.

THEORETICAL

Formulation of Porous Electrode Model

An electrolytic cell having two flow-through porous electrodes separated by a membrane and operated under steady, continuous conditions in a flow-by configuration was investigated. Figure 1 illustrates the cell configuration. The porous electrodes were of uniform porosity, thickness and specific surface area throughout, and were assumed to be made up of a packed bed of spheres. Dilute solution theory was used to describe the transport of species in solution. The kinetic behavior of the electrochemical reactions was represented by the Tafel form of the Butler-Volmer equation. One main electrochemical reaction occurred at each electrode, with oxygen evolution as a side reaction at the anode and hydrogen evolution as a side reaction at the cathode.

The equations representing the system were based on several assumptions: (a) the electrode phase was isopotential; (b) the pores of the electrode were large with respect to the double layer; (c) convection through the porous electrodes occurred by plug flow with no channeling effects; (d) transport through axial diffusion and

dispersion were negligible compared to axial convection; (e) conduction through bulk electrolyte obeys Ohm's law, and migration effects were negligible due to a large excess of supporting electrolyte; (f) mass transfer from the bulk stream to the electrode surface may be characterized by an average mass transfer coefficient which was independent of position; (g) the system was operated isothermally; (h) the conversion per pass was low.

The current balance equation is:

$$\underline{\nabla} \cdot \underline{i} = -a \sum_j f_j^e \tag{1}$$

The rate expression for the main anodic reaction is:

$$f_1^e = i_{01} \frac{c_1^s}{c_1^0} \exp\{\alpha n_1 F \phi^+ / RT\} \tag{2}$$

For the side reaction at the anode, the reaction kinetics is given by:

$$f_2^e = i_{02} \frac{c_2^s}{c_2^0} \exp\{\alpha n_2 F (\phi^+ + \phi_{r1})/RT\} \tag{3}$$

In the above two equations, ϕ^+ is the potential with respect to the thermodynamic rest potential of the main anodic reaction while ϕ_{r1} is the thermodynamic rest potential of the main anodic reaction with respect to the thermodynamic rest potential of the side reaction at the anode. The reaction kinetics for the main cathodic reaction is given by:

$$f_3^e = -i_{03} \frac{c_3^s}{c_3^0} \exp\{-\beta n_3 F \phi^- / RT\} \tag{4}$$

For the side reaction at the cathode, the reaction kinetics is given by:

$$f_4^e = -i_{04} \frac{c_4^s}{c_4^0} \exp\{-\beta n_4 F (\phi^- + \phi_{r2})/RT\} \tag{5}$$

In the above two equations, ϕ^- is the potential with respect to the thermodynamic rest potential of the main cathodic reaction while ϕ_{r2} is the thermodynamic rest potential of the main cathodic reaction with respect to the thermodynamic rest potential of the side reaction at the cathode.

The local concentration difference between the surface of the electrode and the concentration of the bulk electrolyte is related

through the mass transfer coefficient:

$$f_j^e = \frac{n_j F k_i}{s_{ij}} (c_i - c_i^s) \qquad (6)$$

From the assumptions of the model, particularly in that it was a differential reactor, the potential distribution is one-dimensional:

$$\frac{d^2\phi}{dy^2} = \frac{a}{\kappa} \sum_j f_j^e \qquad (7)$$

The model for the porous electrode was completed by the following boundary conditions. For the anode:

$$\text{at } y = 0^+: \quad \frac{d\phi^+}{dy} = -\frac{i}{\kappa_1}$$

$$\text{at } y = H^+: \quad \frac{d\phi^+}{dy} = 0$$

For the cathode:

$$\text{at } y = 0^-: \quad \frac{d\phi^-}{dy} = -\frac{i}{\kappa_2}$$

$$\text{at } y = H^-: \quad \frac{d\phi^-}{dy} = 0$$

The main reaction at the anode represents a hypothetical oxidation reaction involving a two-electron transfer process:

$$2A^- = B + 2e^- \qquad E_1^0 = 0.9 \text{ V}$$

The side reaction at the anode is oxygen evolution and is given by:

$$2H_2O = O_2 + 4H^+ + 4e^- \qquad E_2^0 = 1.229 \text{ V}$$

The main reaction at the cathode represents a hypothetical reduction reaction involving a two-electron transfer process:

$$2C^+ + 2e^- = D \qquad E_3^0 = 0.2 \text{ V}$$

The side reaction on the cathode is hydrogen evolution and is given by:

$$2H^+ + 2e^- = H_2 \qquad E_4^0 = 0.0 \text{ V}$$

Formulation of Objective Function and Constraints

The objective function represents the goal of the optimization.

For example, return on investment, discounted cash flow rate of return on investment, and profit are frequently used as objective functions. Two objective functions were formulated in this study. The first objective was that of maximizing a profit function consisting of total revenue minus total cost on an annual basis. The second objective function was that of maximizing current per unit volume. This is equivalent to maximizing the space-time-yield. In order to relate these objectives to the behavior of the porous electrode modeled in the previous section it is necessary to introduce additional equations in the form of material balances, energy balances, mass transfer correlations, and voltage balances.

The applied current density is:

$$i = I/xy \tag{8}$$

A material balance on the anode for species A is:

$$C_1^0 Q_1 = C_1 Q_1 + \frac{IU_1}{n_1 F} \quad \text{moles/s} \tag{9}$$

A material balance on the anode for water is:

$$\frac{M_1^0}{m_1^0} Q_1 = \frac{M_1}{m_1} Q_1 + \frac{18I\ (1 - U_1)}{1000\ n_2 F} \quad \text{kg/s} \tag{10}$$

A material balance on the cathode for species C is:

$$C_3^0 Q_2 = C_3 Q_2 + \frac{IU_2}{n_3 F} \quad \text{moles/s} \tag{11}$$

A material balance on the cathode for H^+ is:

$$C_4^0 Q_2 = C_4 Q_2 + \frac{I\ (1 - U_2)}{n_4 F} \quad \text{moles/s} \tag{12}$$

The anode volumetric flow rate is:

$$Q_1 = v^+ yz \tag{13}$$

The cathode volumetric flow rate is:

$$Q_2 = v^- yz \tag{14}$$

There are also a number of inequality constraints. Anode and cathode conversion are constrained to be less than or equal to 10%, because of the assumption of low conversion per pass. The membrane

area is set not to exceed a maximum area of 4500 cm (45cm x 100 cm). Upper bounds on the anode and cathode pressure drops are also imposed. The pressure drop is correlated using the Ergun equation [11]. The vapor pressure of water in solution and the vapor pressure of pure water are calculated using the fitted equations of LeRoy et al. [12]. The mass transfer correlation of Wilson and Geankoplis [13] is used. The spheres are assumed to be packed in a hexagonal close packed (hcp) arrangement. The activity coefficient, f_i, was calculated using a Debye-Huckel equation.

The conductivity of the solution has to be corrected for the porous media. The effective conductivity for the porous media is given by [14]:

$$\kappa = \left(\frac{2\varepsilon}{3 - \varepsilon}\right) \kappa_0 \tag{15}$$

The voltage drop across the membrane is calculated by taking into account the resistivity of the membrane, the conductivities of the anolyte and catholyte, as well as the thickness of the membrane. The voltage balance is given by:

$$V = E_1^+ + \phi^+\Big|_{y = 0^+} + V_M - E_3^- - \phi^-\Big|_{y = 0^-} \tag{16}$$

The final model consisted of two nonlinear differential equations, 19 variables, 8 equality constraints, and 5 inequality constraints. The two differential equations were used to solve for the potential distributions ϕ^+ and ϕ^-. The remaining 17 variables used in the optimization are presented in Table 1. Upper and lower bounds were imposed on all these 17 variables. The number of degrees of freedom was determined by the number of variables minus the number of equality constraints. In this study, the total number of degrees of freedom was 9.

Method of Solution

The nonlinear differential equations were solved with a finite difference numerical technique. The nonlinear differential equations were first linearized about a trial solution, and the equations were then written in finite difference form by employing central difference operators. The resulting tridiagonal matrix was then inverted by a modified Gauss-Jordan elimination method with the use of a CDC Cyber 175. Solutions of the equation were obtained when a convergence of 0.01% was achieved by the mesh points during successive iterations.

The optimization problem was solved using a successive quadratic

programming method as implemented in the program SQPHP [15]. Successive quadratic programming was chosen because of its need for fewer function and gradient evaluations, its efficiency, ease of use, and reliability.

In SQPHP, the P equality constraints are used to eliminate some of the variables. This is tantamount to reducing the dimensionality of the problem from N to N-P. The code then solves the original problem by solving a sequence of reduced quadratic programming (QP) subproblems. Details are available in the thesis [10].

In the execution of the optimization runs, a large number of different starting points were used, in an attempt to ensure that a global rather than local optimum was found. A total of 68 optimization runs were made for each objective function. The final program required 32.25 K words of core on the CDC Cyber 175.

RESULTS AND DISCUSSION

The methodology by which the following results were obtained was general enough for it to be applied to any electrolytic cell which can be modeled by a combination of differential and algebraic equations. Hence, the results below are presented to illustrate the types of considerations that can be made with the optimization method presented here. The particular results obtained with the model system were not intended to correspond to a particular application.

A series of case studies was carried out in order to evaluate optimization methodology as well as to explore electrochemical aspects of the problem. The seventeen variables in the optimization problem are listed in Table 1. Table 2 summarizes model parameters used, including physical property data, thermodynamic and kinetic rate constants, mass transfer correlation, as well as economic data. For the case studies here, values of parameters were chosen to be representative of a paired synthesis from aqueous solution of two organic compounds, one valued at about $4/kg and the other about $5/kg.

The simple profit objective function took into consideration power costs as well as market prices of feedstocks and products. Table 3 shows the optimal values together with the initial guesses. These initial guesses represent the starting point in the search for the optimum and they are needed to initialize the program. A total of 68 starting points were tried and several local maxima were found. The best of these local maxima has a maximum profit of $63,419.45/yr with a production rate of 10.1 moles/hr, and corresponds to the optimal values and starting point given in Table 3. Since a large number of different starting points were tried, making it likely that all local maxima were found, one can be reasonably confident, though

not absolutely certain, that this is the global maximum.

It is seen from the optimal results in Table 3 that the dimensions x, y, and z of the porous electrode cell were forced to their upper bounds; this was expected since the objective function did not take into account capital costs. Increasing the dimensions of the cell would mean an increase in production rate and hence, profit. However, as the dimensions of the cell increase, the capital costs associated with the cell also increase. To account for this trade off between increasing production rate and capital cost, a capital cost term incorporating the costs of the material and the labor required for the fabrication of the cell needs to be taken into consideration. Provided estimated or actual cost data are available, this can be incorporated into the optimization scheme with modest effort.

The optimum anodic volumetric flow rate Q_1 was found to exist at the upper bound of the range while the cathodic volumetric flow rate Q_2 was not. It was more profitable to increase the throughput of the anode since the anodic product was more valuable than the cathodic product.

With the simple profit objective function the effect of an increase in energy costs was examined. Alkire, Cera, and Stadtherr [7] had used a different optimization problem to explore how changes in the price of electricity impact on profit and on optimum production rate. As the price increases, the profit and the production rate were found to decline. In the present study the major impact of increasing energy costs was decreasing profits. In the study of Alkire, Cera, and Stadtherr [7], it was found that changes in market prices affect only the optimum value of the objective function and not the optimal operating conditions. The same effect was observed in the present study.

To test the consistency of the methodology further, an objective function was chosen which maximized the current per unit volume. Table 4 shows the optimal values of the variables together with initial guesses. It was found that the optimum value was 0.5 A/cm^3, or 14,000 A/ft^3. Again because a large number of starting points were tried, it is likely that this is the global maximum.

The major differences in the optimal results obtained from the two different objectives as shown in Tables 3 and 4 are in the dimensions of the cell and in the applied current density. In the case of the current per unit volume as objective, the cell dimensions are smaller and the applied current density higher in comparison to the profit as objective case. This is because the energy cost in production is not taken into account in the current per unit volume case.

For the cases investigated, the total CPU time needed to arrive

at the optimum depended on the starting point, and ranged from 1.7 to 40 seconds on a CDC Cyber 175. Of this the time spent in the optimization code ranged from 0.5 to 1.5 seconds; the remainder was spent in solving the differential equations. These results suggested that efficient numerical methods for the solution of the differential equations is critically important. These results also suggested that adroit selection of starting point is important, but that the computational costs of the present model are modest in all cases.

The results of the optimization runs may be reformulated into information such as current efficiency, selectivity, space-time yield, and energy consumption. Table 5 compiles optimal results for the two objectives investigated in this study.

It was found that a temperature rise of about 1.5° C occurred in both cases. Hence, heat transfer was not an important consideration.

Sensitivity of the operating variables was investigated by evaluation of the Lagrange multipliers associated with the optimal solution. The Lagrange multipliers are sensitivity coefficients and are therefore capable of giving an indication of sensitivity. They provide a relative measure of the sensitivity of the objective function with respect to small changes in the constraints. If the objective function is in terms of dollars of profit, then the Lagrange multiplier λ_i may be interpreted as dollars of profit per unit of the i^{th} constraint.

Tables 6 and 7 show the Lagrange multipliers for selected variables for the two objectives investigated in this study. The changes were based on a one percent perturbation of the variables at the optimum. The expected changes in optimal value were calculated by multiplying the Lagrange multipliers by the magnitudes of the change. By this method, it is possible to identify the more sensitive features of the cell from among the large list of input parameters and constraints. This capability should be particularly helpful in the early stages of engineering assessment and development. In the cases studied in this investigation it was found that the sensitive variables were the anodic flow rate and the initial concentration of the anodic reactant with the latter being the most sensitive.

CONCLUSIONS

In this study, a successive quadratic programming technique was used to optimize a model of a porous electrode cell that incorporated current and potential distribution phenomena. The model was prepared for optimization by formulating an objective function as well as a system of equality and inequality constraints that included material balances, charge balances, physical property, and physical limitations.

The model used in this study consisted of two nonlinear differential equations, 19 variables, 8 equality constraints, and 5 inequality constraints. The methodology described here gave the optimal value of all the variables required for optimization of two different objectives: maximum profit based on the prices of chemicals and electrical energy, and maximum current per unit volume. Lagrangian multipliers were used to determine the sensitivity of the constraints to the optimal solution.

The model required the use of certain physical property data such as mass transfer coefficients, density, viscosity, conductivity, vapor pressure, activity, and pressure drop. Membrane transport properties were needed to calculate cell voltage. Physical property data correlations were incorporated wherever possible for determining pressure drop, vapor pressure of water, and correcting conductivities for the effect of porosity. A lack of availability of such auxiliary data may limit the accuracy of any optimization model.

It is recognized that to optimize a process, an entire flowsheet needs to be considered rather than a single cell. It is also recognized that in process optimization, the objective function normally consists of maximizing a rate of return on investment or maximizing venture profit. While rate of return is the final criterion in the assessment of a process, it is sometimes convenient, especially in electrochemical processes to develop a criterion which pertains more closely to the electrolytic process. Hence, for electrolytic processes in the preliminary design stages, high selectivity, space-time yield, chemical yield, or energy yield may be the desired objective. However, in a first generation study such as this, the simple profit function served adequately to illustrate the usefulness and feasibility of the methodology.

Tremendous advances in the modeling of electrochemical systems have been made in recent years. Rigorous electrochemical models based on current and potential distribution phenomena within the cell have increasingly served as guides in the design, scale-up, and optimization of electrochemical cells. The development of digital computers and numerical methods for optimization, as well as the recent progress in the thermodynamics of electrolyte solutions, has paved the way for the use of improved optimization techniques for electrochemical processes. This study attempted to show how state-of-the-art optimization techniques can be applied to cell models to obtain optimal conditions and to provide an estimate of the sensitivity of operating variables. Optimization methods can assist in implementing wise technological changes in the electrochemical process industry.

ACKNOWLEDGMENTS

This work was supported by a grant-in-aid from the Monsanto Company.

NOTATION

The following notation has been used throughout this work:

English Characters:

a	=	specific surface area, cm^{-1}.
c	=	concentration, moles/cm^3.
E^o	=	standard electrode potential, volts.
F	=	Farady's constant, 96,487 Coulombs/g-equivalent.
f^e	=	intrinsic reaction rate, A/cm^2.
f_i	=	activity coefficient of species i.
H^+	=	thickness of anode, cm.
H^-	=	thickness of cathode, cm.
I	=	total cell current, amperes.
i_o	=	exchange current density, A/cm^2.
i	=	applied current density, A/cm^2.
k	=	mass transfer coefficient, cm/s.
M	=	molarity, moles/liter.
m	=	molality, moles/kg H_2O.
n	=	number of electrons in reaction, g-equivalents/mole.
p_w	=	vapor pressure of water, atm.
Q_1	=	anode volumetric flow rate, cm^3/s.
Q_2	=	cathode volumetric flow rate, cm^3/s.
R	=	molar gas constant, 8.3143 J/mole-K.
s_i	=	stoichiometric coefficient.
T	=	temperature, K.
U_1	=	current efficiency of anodic reaction.
U_2	=	current efficiency of cathodic reaction.
V	=	cell voltage, volts.
v^+	=	anolyte velocity, cm/s.
v^-	=	catholyte velocity, cm/s.
x	=	width of porous electrode, cm.
y	=	length of porous electrode, cm.
z	=	thickness of porous electrode, cm.
z_i	=	symbol of electronic charge of species i.

Greek Characters:

α	=	anodic transfer coefficient.
β	=	cathodic transfer coefficient.
ϵ	=	void fraction, cm^3 void space/cm^3 reactor volume.
κ	=	electrolyte conductivity, $(ohm\text{-}cm)^{-1}$.
κ_1	=	anolte conductivity, $(ohm\text{-}cm)^{-1}$.

κ_2 = catholyte conductivity, $(ohm\text{-}cm)^{-1}$.
κ^o = specific conductivity, $(ohm\text{-}cm)^{-1}$.
μ = viscosity of solution, g/cm s.
ϕ_r = potential, volts.
ϕ = potential, volts.
λ = Lagrange multiplier

Superscripts:

o = value at reactor inlet.
s = surface value.

Subscripts:

i = species i.
j = reaction j.
r = reference value.

REFERENCES

1. T. R. Beck, in " Techniques of Electrochemistry", Vol. 3, E. Yeager and A. J. Salkind, Editors, New York, 1978.
2. R. W. H. Sargent, in "Computer Applications to Chemical Engineering", G. V. Reklaitis and R. G. Squires, Editors, ACS Symposium Series, No. 124, ACS, Washington, 1980.
3. A. W. Westerberg, in "Foundations of Computer-Aided Process Design", R. S. H. Mah and W. D. Seider, Editors, Vol. 1, Engineering Foundation, New York, 1981.
4. L. S. Lasdon, and A. D. Waren, Oper. Res., 27, 431 (1979).
5. L. S. Lasdon, in "Foundations of Computer-Aided Process Design", R. S. H. Mah and W. D. Seider, Editors, Vol. 1, Engineering Foundation, New York, 1981.
6. A. D. Waren and L. S. Lasdon, Oper. Res., 28, 1029 (1980).
7. R. C. Alkire, G. D. Cera, and M. A. Stadtherr, J. Electrochem. Soc., 129, 1225 (1982).
8. L. Lasdon, A. D. Waren, A. Jain, and M. Ratner, ACM Trans. Mathematical Software, 4, 34 (1978).
9. R. B. Macmullin, Denki Kagaku, 38, 570 (1970).
10. S. A. Soon, M. S. Thesis, University of Illinois, Urbana, 1983.
11. R. B. Bird, W. E. Stewart, and E. N. Lightfoot, "Transport Phenomena", John Wiley and Sons, New York, 1960.
12. R. L. Leroy, C. T. Bowen, and D. J. Leroy, J. Electrochem. Soc. nou., 127, 1954 (1980).
13. E. J. Wilson and G. C. Geankoplis, Ind. Eng. Chem. Fund., 5, 9 (1966).
14. G. Neale and W. Nader, AIChE J., 19, 112 (1973).
15. H. S. Chen and M. A. Stadtherr, Comput. Chem. Eng., in press (1984).

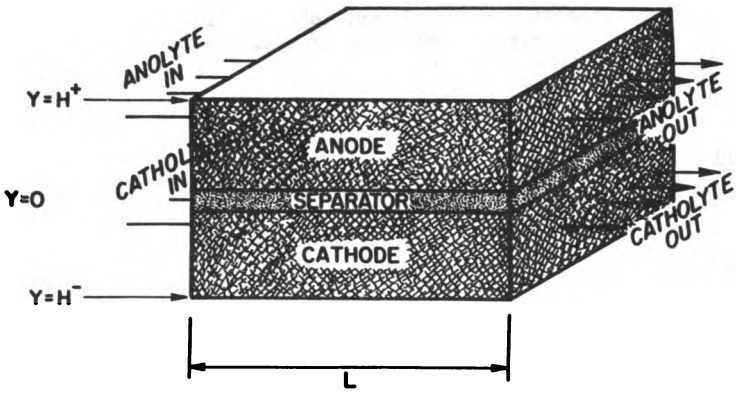

Figure 1: **DIAGRAM OF CELL**

Table 1. Description of Variables in Optimization

VARIABLES	DESCRIPTION
X(1)	TOTAL CELL CURRENT, AMPERES.
X(2)	APPLIED CURRENT DENSITY, AMPERES/CM^2.
X(3)	THICKNESS OF POROUS ELECTRODE, CM.
X(4)	LENGTH OF POROUS ELECTRODE, CM.
X(5)	WIDTH OF POROUS ELECTRODE, CM.
X(6)	ANODIC VOLUMETRIC FLOW RATE, CM^3/S.
X(7)	ANODIC SUPERFICIAL VELOCITY, CM/S.
X(8)	INITIAL CONCENTRATION OF SPECIES 1, MOLES/CM^3.
X(9)	FINAL CONCENTRATION OF SPECIES 1 MOLES/CM^3.
X(10)	CATHODIC VOLUMETRIC FLOW RATE, CM^3/S.
X(11)	CATHODIC SUPERFICIAL VELOCITY, CM/S.
X(12)	INITIAL CONCENTRATION OF SPECIES 3, MOLES/CM^3.
X(13)	FINAL CONCENTRATION OF SPECIES 3, MOLES/CM^3.
X(14)	INITIAL CONCENTRATION OF SPECIES 4, MOLES/CM^3.
X(15)	FINAL CONCENTRATION OF SPECIES 4, MOLES/CM^3.
X(16)	PARTICLE DIAMETER, CM.
X(17)	SPECIFIC SURFACE AREA, 1/CM.

Table 2. Summary of Model Parameters

Input Data

	Anolyte	Catholyte
ρ	1.0056 g/cm^3	1.0061 g/cm^3
μ	0.0114 g/cm s	0.01115 g/cm s
K	0.0515 (ohm-cm)$^{-1}$	0.0552 (ohm-cm)$^{-1}$
	Anode Reaction	**Cathode Reaction**
i_o	2.0 x 10^{-6} A/cm^2	1.4 x 10^{-6} A/cm^2

Other Parameters

α	=	0.5
β	=	0.5
F_1	=	$0.72
F_2	=	$0.53
S_1	=	$3.00
S_2	=	$3.70
ϵ_p	=	0.97
W_1	=	100 g/mole
W_2	=	78 g/mole
W_3	=	50 g/mole
W_4	=	39 g/mole

$K = 1.09 \left(\frac{\epsilon_p}{d_p}\right)^{2/3} G^{1/3}$ cm/s

Selected Upper Bounds:

x	$\leq$	100 cm
y	$\leq$	45 cm
z	$\leq$	4 cm
Q_1	$\leq$	4692 cm^2
Q_2	$\leq$	1 x 10^6 g/cm s^2 (1 atm)

Table 3. Optimal Solution Obtained with Simple Profit as Objective

Variable	Initial Guess	Optimal Value	
I	1172.5056	542.968	Amperes
i	0.2513	0.1206595	A/cm^2
x	1.3125	4.	cm
y	28.75	100.	cm
z	1.5	45.	cm
Q_1	1.5125	270.	cm^3/s
v^+	0.4375	1.5	cm/s
c_1^0	2.5002×10^{-4}	9.104211×10^{-4}	$moles/cm^3$
c_1	2.2502×10^{-4}	9.0×10^{-4}	$moles/cm^3$
Q_2	1.5125	37.98227	cm^3/s
v^-	0.4375	0.2110126	cm/s
c_3^0	2.5002×10^{-4}	9.740788×10^{-4}	$moles/cm^3$
c_3	2.2502×10^{-4}	9.0×10^{-4}	$moles/cm^3$
c_4^0	1.0×10^{-10}	2.346358×10^{-9}	$moles/cm^3$
c_4	9.0×10^{-11}	2.278195×10^{-9}	$moles/cm^3$
d_p	1.0×10^{-3}	9.045099×10^{-3}	cm
a	220.	490.8736	cm^{-1}

Table 4: Optimal solution obtained with current per unit volume as objective

Variable	Initial Guess	Optimal Value	
I	4.5×10^{-3}	1.131184	A
i	$1. \times 10^{-3}$	0.2513743	A/cm^2
x	0.25	0.25	cm
y	3.	3.	cm
z	1.5	1.5	cm
Q_1	1.88×10^{-2}	0.5625	cm^3/s
v^+	5.0×10^{-2}	1.5	cm/s
c_1^0	1.9×10^{-8}	9.104211×10^{-4}	$moles/cm^3$
c_1	1.7×10^{-8}	9.0×10^{-4}	$moles/cm^3$
Q_2	1.88×10^{-2}	5.861846×10^{-2}	cm^3/s
v^-	5.0×10^{-2}	0.1563159	cm/s
c_3^0	1.9×10^{-8}	1.0×10^{-3}	$moles/cm^3$
c_3	1.7×10^{-8}	9.0×10^{-4}	$moles/cm^3$
c_4^0	1.0×10^{-10}	9.683423×10^{-10}	$moles/cm^3$
c_4	9.0×10^{-11}	9.315934×10^{-10}	$moles/cm^3$
d_p	1.0×10^{-3}	1.999999×10^{-2}	cm
a	220.	222.0002	cm^{-1}

	Objective Function	
	Profit	Current per unit volume
Current Efficiency of Anode	100%	99.9999%
Current Efficiency of Cathode	99.9999%	100%
Selectivity of Anode	100%	100%
Selectivity of Cathode	100%	100%
Space-Time Yield	1,105 $\frac{\text{moles}}{\text{liter-hr}}$	1,041 $\frac{\text{moles}}{\text{liter-hr}}$
Energy Consumption	126.5 kwh/kmol	197.3 kwh/kmol

Table 5: Optimal Electrochemical Figures of Merit

Constraints	Lagrangian Multipliers	Units	Change	Expected Change In Optimal Objective
Current Density	-5.1896×10^{-21}	\$/A/cm^2	1.2×10^{-3} A/cm^2	-
Anodic Volumetric Flow Rate	2.3489×10^{2}	\$/cm^3/s	2.7 cm^3/s	\$634.20
Initial Concentration of Anodic Reactant	-6.3923×10^{9}	\$/moles/cm^3	9.1×10^{-6} moles/cm^3	-958,169.00
Cathodic Volumetric Flow Rate	2.273×10^{-13}	\$/cm^3/s	0.38 cm^3/s	-
Initial Concentration of Cathodic Reactant	-2.4758×10^{7}	\$/moles/cm^3	9.7×10^{-6} moles/cm^3	-9240.16
Specific Surface Area	-2.0127×10^{-13}	\$/cm^{-1}	4.9 cm^{-1}	-

Table 6: Lagrange Multipliers for Select Variables Simple Profit as Objective

Constraints	Lagrangian Multipliers	Units	Change	Expected Change In Optimal Objective
Current Density	-1.2632×10^{-16}	A/cm^3/A/cm^2	2.3×10^{-3} A/cm^2	-
Anodic Volumetric Flow Rate	0.8938	A/cm^3/cm^3/s	5.62×10^{-3} cm^3/s	0.005
Initial Concentration of Anodic Reactant	-4.8243×10^{4}	A/cm^3/moles/cm^3	9.1×10^{-6} moles/cm^3	-0.439
Cathodic Volumetric Flow Rate	-2.1907×10^{-16}	A/cm^3/cm^3/s	5.86×10^{-4} cm^3/s	-
Initial Concentration of Cathodic Reactant	2.4209×10^{-6}	A/cm^3/moles/cm^3	1.0×10^{-5} moles/cm^3	-
Specific Surface Area	6.7536×10^{-15}	A/cm^3/cm^{-1}	2.2 cm^{-1}	-

Table 7: Lagrange Multipliers for Select Variables Current per unit Volume as Objective